Opening the Rome-Southampton window for operator mixing matrices

R. Arthur, P. A. Boyle, N. Garron, C. Kelly, and A. T. Lytle (RBC and UKQCD Collaborations)

Phys. Rev. D **85**, 014501 — Published 5 January 2012

DOI: 10.1103/PhysRevD.85.014501

Opening the Rome-Southampton window for operator mixing matrices

R. Arthur,[1] P.A. Boyle,[1] N. Garron,[1] C. Kelly,[2] and A.T. Lytle[3]
(RBC and UKQCD Collaborations)

[1]*SUPA, School of Physics, The University of Edinburgh, Edinburgh EH9 3JZ, UK*
[2]*Physics Department, Columbia University, New York, NY 10027, USA.*
[3]*School of Physics and Astronomy, University of Southampton, Southampton SO17 1BJ, UK*

We show that the running of operators which mix under renormalization can be computed fully non-perturbatively as a product of continuum step scaling matrices. These step scaling matrices are obtained by taking the "ratio" of Z matrices computed at different energies in an RI-MOM type scheme for which twisted boundary conditions are an essential ingredient. Our method allows us to relax the bounds of the Rome-Southampton window. We also explain why such a method is important in view of the light quark physics program of the RBC-UKQCD collaborations. To illustrate our method, using $n_f = 2 + 1$ domain-wall fermions, we compute the non-perturbative running matrix of four-quark operators needed in $K \to \pi\pi$ decay and neutral kaon mixing. Our results are then compared to perturbation theory.

Introduction

Lattice QCD has now reached a stage of high precision in flavour physics and plays a crucial rôle in the quest for new physics. Precision phenomenology requires using a non-perturbative scheme to renormalize quantities obtained from lattice simulations, avoiding ill convergent and low order lattice perturbation theory. One possibility is to use the Schrödinger functional (SF) scheme, a theoretically appealing method which allows for a smooth connection between low energy - where the hadronic matrix elements are computed on the lattice - and very high energy, where the perturbative series is accurate [1, 2]. This connection is done through the use of step-scaling functions [3–5]. Unfortunately, the range of operators actually computed in the SF scheme is rather limited; perhaps this is due to the fact that a peculiar perturbation theory (different from the infinite volume one) is required. Another possibility - very popular in the lattice community - is to use a RI-MOM type scheme [6]: such a scheme is theoretically sound, relatively easy to implement and the connection to $\overline{\rm MS}$ or any other perturbative scheme is done using continuum infinite volume perturbation theory. Thus one benefits from the recent multi-loop computations achieved by several groups (see for example [7–9]). In an RI-MOM type scheme one numerically computes the off-shell amputated vertex function $G_{\rm O}$ of the operator of interest O between external states with given momenta and fixed gauge gluonic configurations. We project this quantity onto its Dirac-colour structure and obtain the quantity $\Lambda_{\rm O}$ (the choice of projector is in general not unique and the precise definition of the scheme depends on this choice of projector). We take all the quark masses to be degenerate and equal to m. Then one requires that in the chiral limit the renormalized projected-amputated operator matches its tree-level value [6], i.e. if a is the lattice spacing, n is the number of quark fields, ψ, in the operator and μ is the renormalization scale (which depends on the choice of external momenta), and F is the tree level value of $\Lambda_{\rm O}$, one imposes

$$Z_O^{\mathcal{S}}(\mu, a)\; Z_\psi^{-n/2}(\mu, a) \lim_{m\to 0} \Lambda_{\rm O}(\mu, a, m) = F\;. \qquad (1)$$

In this way one obtains, non-perturbatively, the scheme and scale dependent renormalization factors $Z_O^{\mathcal{S}}(\mu, a)$. The precise definition of the lattice scheme $\mathcal{S}$ depends on the details of the implementation. In the second step, one converts the result to a scheme more appropriate for phenomenological applications. In the case of an effective low-energy theory one can express the Hamiltonian by a sum of local operators multiplied by some Wilson coefficients. One must find a scheme where both the renormalized matrix elements of these operators and the corresponding Wilson coefficients can be computed. Typically, one matches the Z factors obtained in the lattice scheme at $\mu \sim 2-3$ GeV to $\overline{\rm MS}$. Equivalently, (if perturbation theory is accurate) one can divide the vertex function computed in the lattice scheme by the corresponding running to obtain the renormalization group invariant Z factor and then convert to the desired scheme and scale. It is important to note that the running and the matching are usually computed only perturbatively (we discuss some recent implementations of a non-perturbative running in the next section).

In order to keep the discretisation effects under control, and at the same time access a region where perturbation theory can be applied, RI-MOM schemes require the existence of the so-called Rome-Southampton window: ideally one would require $\Lambda_{\rm QCD} \ll \mu \ll a^{-1}$. In practice, this window can be quite narrow or even closed and most of the lattice computations are done with $a\mu \sim 1$. In fact the size of the discretisation effects depends on the lattice action, and it is usually admitted that for an off-shell O(a)-improved action it is sufficient to require $(a\mu/\pi)^2 \ll 1$. Concerning the other side of the window the situation was greatly improved when it was realised that a different choice of kinematics, called non-exceptional, strongly suppresses some infrared contributions to the vertex function [10, 11]. Nevertheless,

this window is still an important limitation, in particular when considering light pion masses where the physical volume - and thus the lattice spacing - has to be large. This could become a real issue when one tries to tackle the very challenging computation of $K \to \pi\pi$ decays because one needs even larger physical volumes. A new step scaling method has recently been introduced [12] that allows to address the window problem for RI-MOM. This method has already been applied for multiplicatively renormalized operators [13, 14].

Strategy

In this work we apply the method presented in [12], generalised to the case where several operators mix under renormalization. The main idea is to separate the scale and the lattice spacing(s) at which the bare matrix elements are computed from the ones at which the running and the conversion to the perturbative scheme are performed. Let us consider the case of four-quark operators mixing: following again [6], we define a matrix of amputated, projected vertex functions $\Lambda_{ij} = P_j\{G_{O_i}\}$, where the O_i form a basis under renormalization and the P_i projects and traces onto the Dirac-colour structure of the corresponding operator O_i. If we denote by F the tree-level value of Λ, equation (1) becomes

$$\frac{Z_{ij}^{\mathcal{S}}(\mu,a)}{Z_{\rm A}(a)^2} \times \lim_{m\to 0} \frac{\Lambda_{jk}(\mu,a,m)}{\Lambda_{\rm A}(\mu,a,m)^2} = F_{ik} \ , \qquad (2)$$

where, for convenience, we use the vertex function of the axial current $\Lambda_{\rm A}$ to fix Z_ψ. Equation (2) defines $Z_{ij}^{\mathcal{S}}$ where the scheme $\mathcal{S}$ depends on the choice of kinematics and projectors of the four-quark vertex function and on the choice of quark wave function renormalization [13]. At finite lattice spacing a and for a given renormalization scale μ we consider the matrix

$$R_{\mathcal{S}}(\mu,a) = \lim_{m\to 0} \left[\Lambda_{\rm A}^2(\mu,a,m)\,\Lambda^{-1}(\mu,a,m)\right] \ , \qquad (3)$$

and we define the step scaling matrix by

$$\sigma^{\mathcal{S}}(\mu,s\mu) = \lim_{a\to 0} \Sigma^{\mathcal{S}}(\mu,s\mu,a) = \lim_{a\to 0} \left[R_{\mathcal{S}}(\mu,a) R_{\mathcal{S}}^{-1}(s\mu,a)\right] \ . \qquad (4)$$

We also note that $Z_{\rm A}(a)$ cancels out in the ratio since, to a very good approximation, it does not depend on the scale μ. One important point is that although the quantities Λ, Z and R depend on the details of the computation this is not the case for the step scaling matrix which has well-defined continuum limit and depends only on the choice of renormalization scheme $\mathcal{S}$ (and on the number of flavours). In this work we use a scheme which is called (γ_μ,γ_μ)-scheme in [13]: it involves non-exceptional kinematics with a symmetric point. Such a choice greatly suppresses unwanted infrared effects.

The strategy that we are proposing can be summarised in the following way:

- Consider a set of simulations with a rather large volume of spatial extent L_0 where physical pion masses can be simulated and with moderately large lattice spacings a_0, but small enough for the Symanzik expansion to converge. Compute the bare matrix elements of interest $\langle \mathcal{O}^{\rm bare}(a_0)\rangle$ and renormalize them in a lattice scheme $\mathcal{S}$ at the low energy scale μ_0, i.e. compute $\langle \mathcal{O}^{\mathcal{S}}(\mu_0)\rangle = \lim_{a_0\to 0}\left[Z_{\mathcal{O}}^{\mathcal{S}}(\mu_0,a_0)\langle \mathcal{O}^{\rm bare}(a_0)\rangle\right]$. Of course the scale μ_0 should be such that the associated discretisation errors are small but, compared to the Rome-Southampton window, we do not require the non-perturbative effects to be small. Instead one just has to ensure that the finite volume effects are negligible, so the renormalization window becomes

$$L_0^{-2} \ll \mu_0^2 \ll (\pi/a_0)^2 \ .$$

- Iterate the following step, with $\mathrm{i} = 1,2,\ldots,\mathrm{n}$: consider a set of simulations, with a physical volume of space extent $L_{\rm i} < L_{\rm i-1}$ and a set of lattice spacings a_i. With the requirement that, on each lattice,

$$L_{\rm i}^{-2} \ll \mu_{\rm i-1}^2 < \mu_{\rm i}^2 \ll (\pi/a_{\rm i})^2$$

  is satisfied, compute the step scaling matrix by evaluating eq. (4).

- At a scale $\mu_{\rm n}$ high enough to apply perturbation theory, multiply by the perturbative matching and running factors corresponding to the desired scale and scheme (typically $\overline{\rm MS}$ at $\mu = 2$ or $\mu = 3$ GeV). In this volume the usual Rome-Southampton condition holds

$$\Lambda_{\rm QCD}^2 \ll \mu_{\rm n}^2 \ll (\pi/a_{\rm n})^2 \ .$$

In summary, the general equation can be written as

$$\langle O^{\overline{\rm MS}}(\mu)\rangle = C^{\overline{\rm MS}\leftarrow\mathcal{S}}(\mu) \times U^{\mathcal{S}}(\mu,\mu_{\rm n}) \times \underbrace{\sigma^{\mathcal{S}}(\mu_{\rm n},\mu_{\rm n-1})}_{\text{Fine lattices}} \times \sigma^{\mathcal{S}}(\mu_{\rm n-1},\mu_{\rm n-2}) \times \ldots \times \sigma^{\mathcal{S}}(\mu_1,\mu_0) \times \underbrace{\langle O^{\mathcal{S}}(\mu_0)\rangle}_{\text{Coarse lattices}} \ , \qquad (5)$$

where $C^{\overline{\rm MS}\leftarrow\mathcal{S}}(\mu)$ represents the matrix of matching factors which converts the Z matrix computed in the

scheme $\mathcal{S}$ to the scheme $\overline{\text{MS}}$, and $U^{\mathcal{S}}(\mu, \mu_{\text{n}})$ is the usual running matrix in the scheme $\mathcal{S}$ computed in perturbation theory. In the previous equation we have made explicit the fact that our method consists in re-expressing the running matrix, usually computed in perturbation theory, by a product of continuum non-perturbative step scaling matrices.

One notices that in the first n−1 steps, the lower bound of the Rome-Southampton window (Λ_{QCD}) is replaced by a more advantageous one (L_i^{-1}). In other words: we do not need to be in the perturbative regime. Moreover a better control of the upper bound is achieved by taking the continuum limit of the step scaling function (in particular there is no discretisation error of order $a_0^2\mu_{\text{n}}^2$ in contrast to the "naive" RI-MOM implementation). A couple of remarks are in order:

- Using twisted boundary conditions circumvents the Fourier mode constraints and allows us to fix the orientation of the momentum while changing its magnitude. As emphasised in [12], thanks to this property we can compute the vertex functions for an arbitrary number of points lying on the same scaling trajectory. The continuum limit of the vertex function as a function of μ^2 is then properly defined and in particular we do not need to perturbatively subtract any lattice artefact. The continuum extrapolation is also easier since, if we know the lattice spacings with sufficient precision, we can simulate any arbitrary momentum. This is also useful because our method requires that each momentum $p = \mu_0, \mu_1, \ldots \mu_{\text{n}}$ has to be common to different sets of lattices.

- Since we impose periodic boundary conditions, one could worry about the use of perturbation theory in a small volume, where the space extent is of the order of (or smaller than) $\Lambda_{\text{QCD}}^{-1}$ [15]. However we claim that in a non-exceptional graph with hard external momenta, decoupling will ensure, for $\mu \gg L^{-1}$, that our computation is free from finite volume effects and finite volume perturbation theory is not needed. While this might need further investigation, it is not relevant here since we consider only "infinite" volumes (of spatial extent much larger than $\Lambda_{\text{QCD}}^{-1}$).

Before closing this section we wish to mention other works on non-perturbative running in RI-MOM. Taking the continuum limit of the ratio of Z factors at different energies in an RI-MOM scheme was first proposed in [16] but the authors did not address how to match the momenta computed with different lattice spacings such that the lattice artefacts have an a^2 expansion. Zhestkov [17] used fine tuning of β in the quenched approximation to exactly match the Fourier modes but did not define a quantity which has a well-defined continuum limit. More recent work has looked at the ratios of Zs [14, 18, 19]. However, how to continuum extrapolate the distinct Fourier modes with distinct lattice artefacts must be addressed. Some cases have model input like perturbative subtraction of the lattice discretisation effects, or rules of thumb such as use of $\sin(p)$ instead of p. Instead here we follow [12] and implement twisted boundary conditions to keep the orientation of the momenta fixed and give the observables a smooth a^2 dependence, and allow for a full non-perturbative continuum extrapolation.

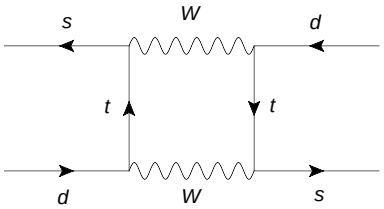

FIG. 1: Example of box diagram contributing to $K^0 - \overline{K^0}$ mixing in the Standard model.

Renormalization of kaon weak matrix elements. In this section we give the definitions of the kaon four-quark operators that we consider in this work. We refer the reader who would like to find more details about this part to the recent reviews [20, 21].

In the standard model, neutral kaon mixing is dominated by box diagrams like the one shown in figure 1. The non-perturbative contributions are given by $\langle \overline{K}^0 | O^{\Delta s=2}_{\text{VV+AA}} | K^0 \rangle$, where $O^{\Delta s=2}_{\text{VV+AA}}$ is the parity conserving part of $(\overline{s}\gamma_\mu(1-\gamma_5)d)(\overline{s}\gamma_\mu(1-\gamma_5)d)$. It is well known that this operator belongs to the (27,1) representation of $SU(3)_{\text{L}} \times SU(3)_{\text{R}}$ and renormalizes multiplicatively. To study neutral kaon mixing beyond the standard model it is useful to introduce the so-called SUSY basis of $\Delta s = 2$ operators. In this basis $O_1^{\Delta s=2}$ is the standard model operator, $O_i^{\Delta s=2}$, $i > 1$ are beyond the standard model (BSM) operators. Denoting by α and β the colour indices, one has

$$
\begin{aligned}
(27,1) \qquad & O_1^{\Delta s=2} = (\overline{s}_\alpha \gamma_\mu (1-\gamma_5) d_\alpha)\,(\overline{s}_\beta \gamma_\mu (1-\gamma_5) d_\beta)\,, \\
(6,\overline{6}) \qquad & \begin{cases} O_2^{\Delta s=2} = (\overline{s}_\alpha (1-\gamma_5) d_\alpha)\,(\overline{s}_\beta (1-\gamma_5) d_\beta)\,, \\ O_3^{\Delta s=2} = (\overline{s}_\alpha (1-\gamma_5) d_\beta)\,(\overline{s}_\beta (1-\gamma_5) d_\alpha)\,, \end{cases} \\
(8,8) \qquad & \begin{cases} O_4^{\Delta s=2} = (\overline{s}_\alpha (1-\gamma_5) d_\alpha)\,(\overline{s}_\beta (1+\gamma_5) d_\beta)\,, \\ O_5^{\Delta s=2} = (\overline{s}_\alpha (1-\gamma_5) d_\beta)\,(\overline{s}_\beta (1+\gamma_5) d_\alpha)\,. \end{cases}
\end{aligned}
$$

The operators have been studied with various lattice formulations, see for example [22–24]. As we wrote explicitly in the previous equations, $O_2^{\Delta s=2}$ and $O_3^{\Delta s=2}$ transform like $(6,\overline{6})$ under $SU(3)_{\text{L}} \times SU(3)_{\text{R}}$ and then mix together under renormalization. Likewise $O_4^{\Delta s=2}$ and $O_5^{\Delta s=2}$ belong to $(8,8)$ and also mix together. Thus in a scheme which preserves chiral symmetry the five-by-five renormalization matrix is block diagonal: the only

non-zero Z factors can be divided in three subgroups: a single factor for the $(27,1)$ operator and two, two-by-two matrices for the BSM operators. In practice it is convenient to work in another basis where all the operators are colour unmixed and we consider only the parity even component of the four-quark operators. Using the notation $\Gamma \otimes \Gamma \to (\overline{s}_\alpha \Gamma d_\alpha)\,(\overline{s}_\beta \Gamma d_\beta)$ we define the renormalization basis by:

$$
\begin{aligned}
(27,1) \qquad & Q_1^{\Delta s=2} = \gamma_\mu \otimes \gamma_\mu + \gamma_\mu\gamma_5 \otimes \gamma_\mu\gamma_5\,, \\
(8,8) \qquad & \begin{cases} Q_2^{\Delta s=2} = \gamma_\mu \otimes \gamma_\mu - \gamma_\mu\gamma_5 \otimes \gamma_\mu\gamma_5\,, \\ Q_3^{\Delta s=2} = \mathrm{I} \otimes \mathrm{I} - \gamma_5 \otimes \gamma_5\,, \end{cases} \\
(6,\overline{6}) \qquad & \begin{cases} Q_4^{\Delta s=2} = \mathrm{I} \otimes \mathrm{I} + \gamma_5 \otimes \gamma_5\,, \\ Q_5^{\Delta s=2} = \sigma_{\mu\nu} \otimes \sigma_{\mu\nu}\,. \end{cases}
\end{aligned}
$$

The explicit relations between the two bases are given in the appendix. We denote by $Z^{\Delta s=2}$ the (block diagonal) renormalization matrix defined in the renormalization basis.

It is interesting to note that the renormalization factors of some $\Delta s = 1$ operators which appear in $K \to \pi\pi$ decays can be obtained from those of the $\Delta s = 2$ operators mentioned above. At low energy in the $\Delta I = 3/2$ channel they are three operators that contribute: a $(27,1)$ called $Q'^{\Delta s=1,\Delta I=3/2}_1$ which renormalizes multiplicatively and two $(8,8)$ which mix together: the electroweak penguins $Q'^{\Delta s=1,\Delta I=3/2}_{7,8}$. We give the explicit form of these operators in the appendix. Denoting by $\mathcal{Z}^{\Delta s=1}_{ij}, \quad i,j = 1,7,8$ the corresponding renormalization factors, the relation to the $Z^{\Delta s=2}_{ij}$ reads

$$
\begin{array}{rclcrcl}
 & & & & \mathcal{Z}^{\Delta s=1}_{11} & = & Z^{\Delta s=2}_{11}\,, \\
\mathcal{Z}^{\Delta s=1}_{77} & = & Z^{\Delta s=2}_{22}\,, & & \mathcal{Z}^{\Delta s=1}_{78} & = & -\tfrac{1}{2}\, Z^{\Delta s=2}_{23}\,, \\
\mathcal{Z}^{\Delta s=1}_{87} & = & -2\, Z^{\Delta s=2}_{32}\,, & & \mathcal{Z}^{\Delta s=1}_{88} & = & Z^{\Delta s=2}_{33}\,.
\end{array}
$$

In this work we give some results for the non-perturbative running of $Q^{\Delta s=2}_{i=1,\ldots 5}$ and $Q'^{\Delta s=1,\Delta I=3/2}_{1,7,8}$. A full computation of $K \to \pi\pi$ decays requires also the renormalization of $\Delta I = 1/2$ four-quark operators which transform like $(8,1)$ under $SU(3)_\mathrm{L} \times SU(3)_\mathrm{R}$. Because for these operators one has to compute disconnected diagrams we do not consider them in this work and leave them for the future. Although these operators are important in a full computation of $K \to \pi\pi$ amplitudes the main purpose of this paper is to give a method for a computation of a non-perturbative running in the operators mixing case. Furthermore the operators that we consider here already have an important phenomenological relevance since they allow for the computation of standard model and beyond the standard model neutral kaon mixing matrix elements and of $K \to \pi\pi$ amplitude in the $\Delta I = 3/2$ channel.

Numerical application

The RBC-UKQCD collaboration has recently performed a computation of $K \to \pi\pi$ decay amplitudes (in both isopsin channels) with a two-pion final state [25]. The physical matrix elements are computed from the Euclidean ones by using the Lellouch-Lüscher formula [26]. The results are very promising but, since it was the first computation of its kind, an unphysical pion mass of $m_\pi \sim 422\,\mathrm{MeV}$ was used. In order to simulate the physical kinematics the collaboration is currently repeating the computation on a much larger volume - of spatial extent $L_0 \sim 4.6\,\mathrm{fm}$ - with a nearly physical pion mass of $m_\pi \sim 140$ MeV. Some promising preliminary results of the $K \to \pi\pi$ matrix elements in the $\Delta I = 3/2$ channel have been reported in [27]. The gauge action used is a modification of the Iwasaki gauge action following the lines of [28, 29], that we call the "dislocation suppressing determinant ratio". On the same lattice, a computation of the matrix element $\langle \overline{K}^0 | O^{\Delta s=2}_{\mathrm{VV+AA}} | K^0 \rangle$ is also on the way. With a lattice spacing $a_0 \sim 0.14\,\mathrm{fm}$ one might worry about the size of the discretisation effects for a momentum of two or three GeV (indeed one might doubt the existence of the Rome-Southampton window on this lattice). The way out is to follow the strategy explained in the previous section with $n = 1$ (two different physical volumes). Firstly, in the volume L_0 we compute the bare matrix elements and the renormalization factors at a low energy μ_0, where we use $\mu_0 \sim 1.5\,\mathrm{GeV}$. Then the continuum limit of the step scaling matrix $\sigma(\mu_1, \mu_0)$, with $\mu_1 \in [\mu_0, 3\,\mathrm{GeV}]$ is obtained from another set of simulations. There we use $L_1 \sim 2.7\,\mathrm{fm}$ and two finer lattice spacing $a_1 \sim 0.086\,\mathrm{fm}$ and $0.114\,\mathrm{fm}$ (more details about these simulations can be found in [30, 31]). Finally we plan to combine the two results in order to compute the renormalized matrix element at 2 or 3GeV and then apply the perturbative matching to $\overline{\mathrm{MS}}$. As mentioned above the two different volumes use two different gauge actions but the results can be combined together because we extrapolate the step

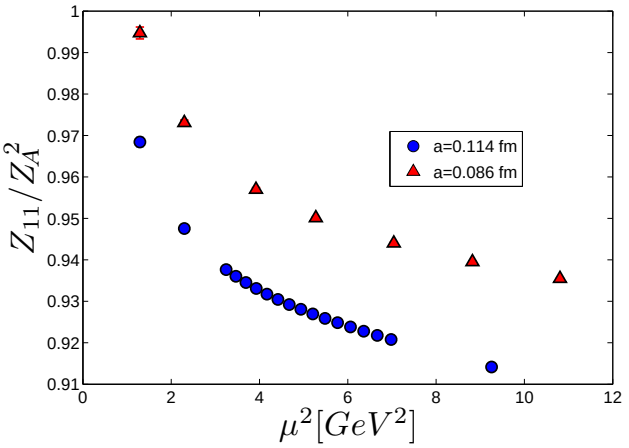

FIG. 2: Renormalization factor $Z_{11}/Z_\mathrm{A}^2 = Z_{\mathrm{B_K}}$, obtained at two different values of the lattice spacing. Except for a few points, the error bars are smaller than the symbols.

scaling matrix to the continuum. Although in principle we would like to have a third lattice spacing in order to have a better control on the continuum extrapolations in the volume L_1, in practice the discretisation effects on the step scaling matrix elements appear to be small. Obviously this method can be applied to all sort of different quantities that one would like to extract from our large lattice L_0. In the near future, when the next generation of supercomputers will be available, we plan to add a finer lattice on the large volume L_0.

In the rest of this section we present our results for the step scaling matrices $\sigma(\mu_0, \mu)$ with μ varying in a range $[\mu_0, \sim 3\,\mathrm{GeV}]$. The computation of the renormalization factors on the fine lattice is done using the same setup as in [13, 32], to which we refer the reader for a more detailed explanation. The computation of the Z factors has been already presented in [32]. One of the main features of our computation is the use of the Domain-Wall fermion [33–35] which exhibits an almost exact chiral-flavour symmetry. As a consequence the renormalization pattern is the same as in the continuum (up to some numerically irrelevant lattice artefacts). Some other interesting aspects of our calculation are the use of the volume sources [36] giving us a very good statistical precision, non-exceptional kinematics [10, 11] to suppress the Goldstone pole contributions: here we use a scheme which is called (γ_μ, γ_μ)-scheme in [13]. In figure 2 we show the Z factor of the $(27, 1)$ operator, normalized by Z_{A}^2 and extrapolated to the chiral limit, obtained on the two different lattices at the simulated momenta (covering a range from $\sim 1.1\,\mathrm{GeV}$ to $\sim 3.5\,\mathrm{GeV}$). The corresponding step scaling function is computed according to the definition eq (4). In figure 3 (left) we plot the result at finite lattice spacing, together with the continuum extrapolation. In order to determine the vertex function at any given momentum for each ensemble we fit our data as a function of p^2 and interpolate. As explained earlier in the text, because we are using twisted boundary conditions that keep the momentum orientation fixed with respect to the lattice axes this is a smooth interpolation. Having obtained in this way the vertex function on a number of lattice spacings at a fixed physical p^2 we extrapolate this to the continuum limit using a constant plus $O(a^2)$ ansatz for each value of the momentum. This ansatz is justified in our approach because as we pick a fixed momentum orientation with respect to the lattice axes, $O(4)$ breaking lattice artefacts are well parametrised [12]. As one can see on the plot, the lattice spacing dependence is very well under control. In [32] we have shown that the renormalization pattern is the same as in the continuum, the chirally forbidden renormalization factors being zero within error. The chiral extrapolation is done using three different quark masses and we found a very mild quark mass dependence for all our quantities. In our setup the sea quark mass of the strange is fixed (to its physical value), whereas the valence sea quarks masses are equal to the sea light quark masses and then extrapolated to zero. As a consequence our results are affected by a small systematic error, which was evaluated in [13] for the $(27, 1)$ operator. We have checked that taking the chiral extrapolation of the ratio of Z gives the same result as taking the ratio of the chiral extrapolation of Z. In figure 3 (right) we compare our non-perturbative result with the next-to-leading order (NLO) running [13]. We note that the running is quite small ($\sim 4\%$ between $\mu \sim 1.5\,\mathrm{GeV}$ and $\sim 3.5\,\mathrm{GeV}$), while NLO perturbation theory predicts $\sim 7\%$. With our very small error bars such a the difference is clearly visible. In figure 4, we plot our results for the two (continuum) two-by-two step scaling matrices $\sigma(\mu, \mu_0)$ computed in the renormalization basis. By definition, at the matching point $\mu = \mu_0$ the matrices are equal to the identity. In figure 5 we compare our results for the electroweak penguins in the $\Delta s = 1$ basis to the next-to-leading order (NLO) running recently computed in [37]. In Figure 6 and 7 we set $\mu_0 = 3\mathrm{GeV}$ and plot the non-perturbative running divided by the NLO prediction. In general we find that when NLO perturbation theory is available the results agree qualitatively with the non-perturbative ones. It is interesting to note that for both the $(8, 8)$ and the $(6, \bar{6})$, we found that one off-diagonal matrix element has a very small non perturbative running, and that the corresponding one loop anomalous dimension is either zero (for σ_{32}) or a very small number (for σ_{45}).

Conclusion

We have presented a general method to compute the non-perturbative continuum running in the operator mixing case. In particular this method allows the use of an RI-MOM type scheme on a rather coarse lattice. We have computed this running between $\sim 1.5\,\mathrm{GeV}$ and $\sim 3.5\,\mathrm{GeV}$ in the case of four-quark operators which occur in neutral kaon mixing (including the BSM ones) and $\Delta I = 3/2$ $K \to \pi\pi$ decays. Although the strategy we have presented is very general we have shown why it is important for the light quark physics program of the RBC-UKQCD collaboration and in particular for a full computation of $K \to \pi\pi$ amplitudes.

Acknowledgments

We thank our colleagues in the RBC and UKQCD collaborations, in particular Norman Christ, Christoph Lehner, and Chris Sachrajda for suggestions and stimulating discussions. The calculations reported here were performed on the QCDOC computers [38, 39] at Columbia University, Edinburgh University, and at Brookhaven National Laboratory (BNL), Argonne Leadership Class Facility (ALCF) BlueGene/P resources at Argonne National Laboratory (ANL), and also the resources of the STFC-funded DiRAC facility. We wish to acknowledge support from STFC grant ST/H008845/1, DOE grant DE-FG02-92ER40699 and to EU grant 238353 (STRONGnet). R.A. is supported by SUPA prize studentship.

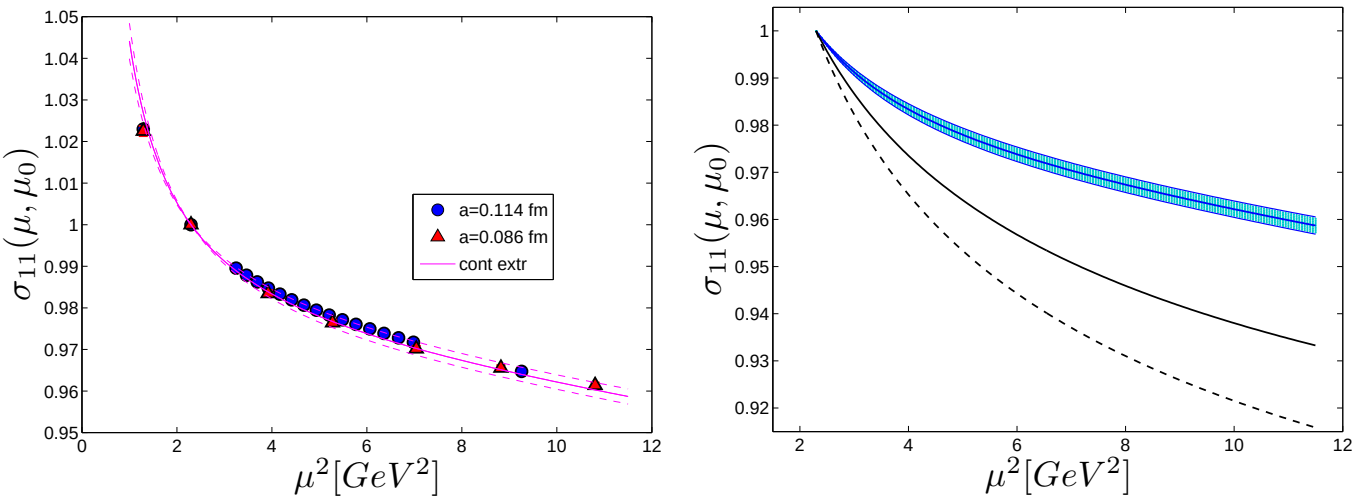

FIG. 3: Left: step scaling function (non-perturbative running) of the $(27,1)$ operator at finite lattice spacings and in the continuum in the lattice SMOM (γ_μ,γ_μ)-scheme . The energy scale μ_0 is fixed to $\mu_0 \sim 1.5\,\mathrm{GeV}$, and μ varies in the range $[1.\,\mathrm{GeV}, \sim 3.5\,\mathrm{GeV}]$. The errors bars are smaller than the symbols. Right: the same quantity is compared to perturbation theory (dashed black curve : one loop, solid black curve: two loops, solid blue curve: continuum extrapolation of non-perturbative running with its error) in the range $[\mu_0, \sim 3.5\,\mathrm{GeV}]$.

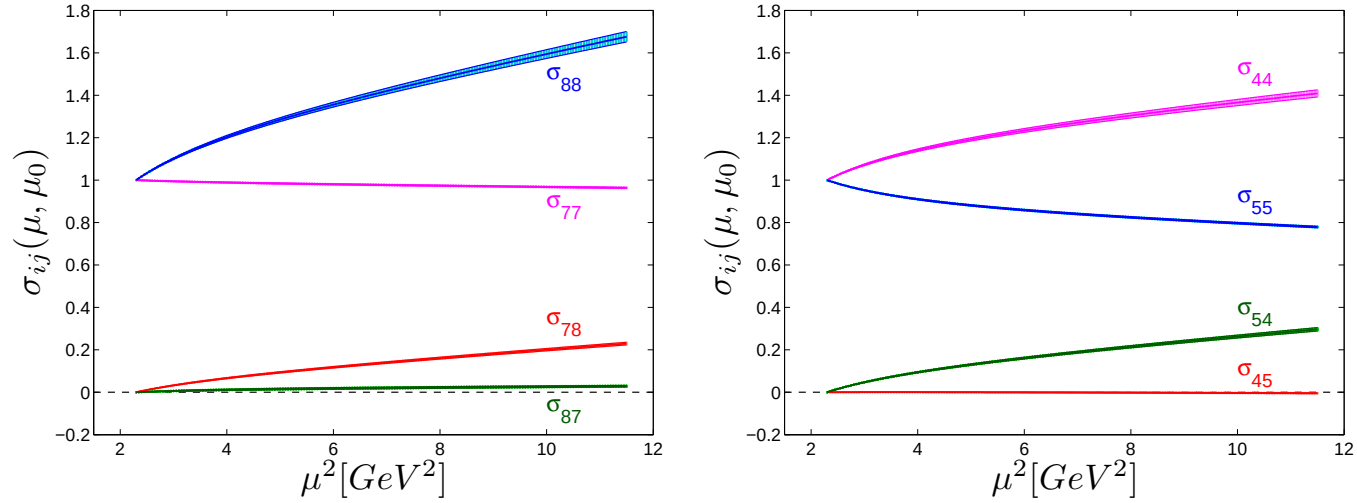

FIG. 4: Step scaling matrix $\sigma(\mu,\mu_0)$ given in the $\Delta s = 2$ renormalization basis. On the left panel we show the matrix elements of the $(8,8)$ operators and on the right the $(6,\bar{6})$ operators. Like in figure 3, the energy scale μ_0 is fixed to $\mu_0 \sim 1.5\,\mathrm{GeV}$, and μ varies in the range $[\mu_0, \sim 3.5\,\mathrm{GeV}]$.

Appendix

1. Denoting by the superscript "+" the parity even component, the explicit relation between the two $\Delta s = 2$ basis is

$$(27,1) \qquad \left[O_1^{\Delta s=2}\right]^+ = Q_1^{\Delta s=2}\,,$$

$$(6,\overline{6}) \quad \begin{cases} \left[O_2^{\Delta s=2}\right]^+ &= Q_4^{\Delta s=2}\,, \\ \left[O_3^{\Delta s=2}\right]^+ &= -\frac{1}{2}(Q_4^{\Delta s=2} - Q_5^{\Delta s=2})\,, \end{cases}$$

$$(8,8) \quad \begin{cases} \left[O_4^{\Delta s=2}\right]^+ &= Q_3^{\Delta s=2}\,, \\ \left[O_5^{\Delta s=2}\right]^+ &= -\frac{1}{2}Q_2^{\Delta s=2}\,. \end{cases}$$

2. To define the $\Delta I = 3/2$ part of the $\Delta s = 1$ operators, we follow the conventions of [40]

$$Q'_1 = (\bar{s}_\alpha\gamma_\mu(1-\gamma_5)d_\alpha)\big[(\bar{u}_\beta\gamma_\mu(1-\gamma_5)u_\beta) - (\bar{d}_\beta\gamma_\mu(1-\gamma_5)d_\beta)\big] + (\bar{s}_\alpha\gamma_\mu(1-\gamma_5)u_\alpha)(\bar{u}_\beta\gamma_\mu(1-\gamma_5)d_\beta)) \quad \text{(A.1)}$$

$$Q'_7 = (\bar{s}_\alpha\gamma_\mu(1-\gamma_5)d_\alpha)\big[(\bar{u}_\beta\gamma_\mu(1+\gamma_5)u_\beta) - (\bar{s}_\beta\gamma_\mu(1+\gamma_5)s_\beta)\big] + (\bar{s}_\alpha\gamma_\mu(1-\gamma_5)u_\alpha)(\bar{u}_\beta\gamma_\mu(1+\gamma_5)d_\beta)) \quad \text{(A.2)}$$

$$Q'_8 = (\bar{s}_\alpha\gamma_\mu(1-\gamma_5)d_\beta)\big[(\bar{u}_\beta\gamma_\mu(1+\gamma_5)u_\alpha) - (\bar{s}_\beta\gamma_\mu(1+\gamma_5)s_\alpha)\big] + (\bar{s}_\alpha\gamma_\mu(1-\gamma_5)u_\beta)(\bar{u}_\beta\gamma_\mu(1+\gamma_5)d_\alpha)) \quad \text{(A.3)}$$

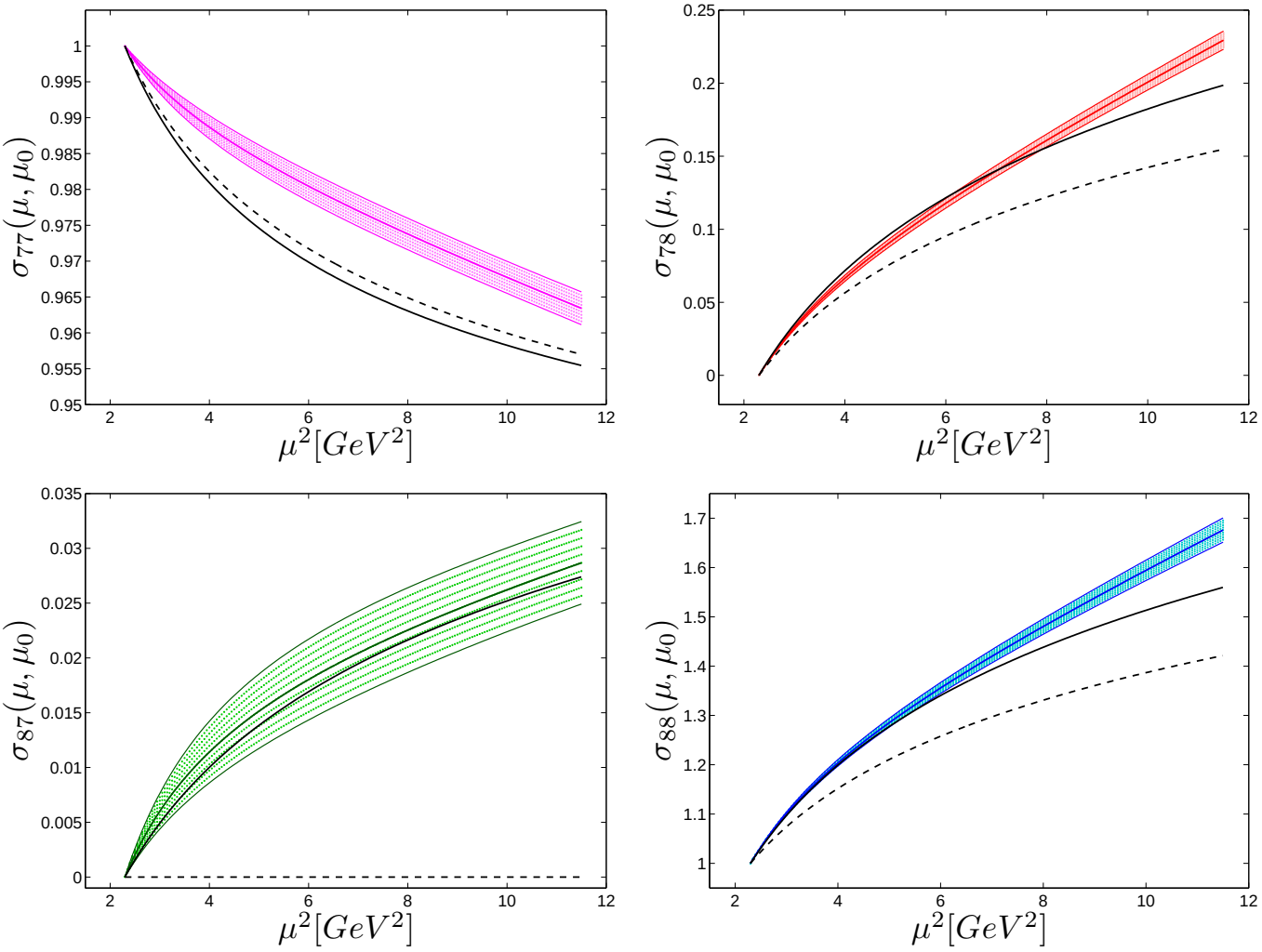

FIG. 5: Step scaling matrix $\sigma(\mu,\mu_0)$ of the $(8,8)$ electroweak penguins in the $\Delta s = 1$ renormalization basis. For each matrix element we compare to perturbation theory (dashed black curve : one loop, solid black curve: two loops, solid coloured curve: continuum extrapolation of non-perturbative running with its error).

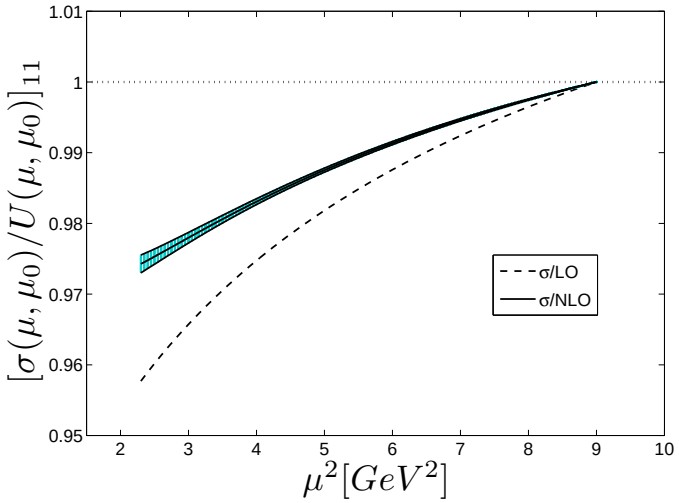

FIG. 6: Step scaling function $\sigma_{11}(\mu,\mu_0)$ of the $(27,1)$ operator divided by the corresponding perturbative running $U_{11}(\mu,\mu_0)$ (dashed line: one loop, solid coloured curve: two loops). For ease of comparison with perturbation theory and in contradiction to the previous plots, μ_0 is fixed at the conventional scale of 3 GeV and μ varies in the range [1.5 GeV, μ_0].

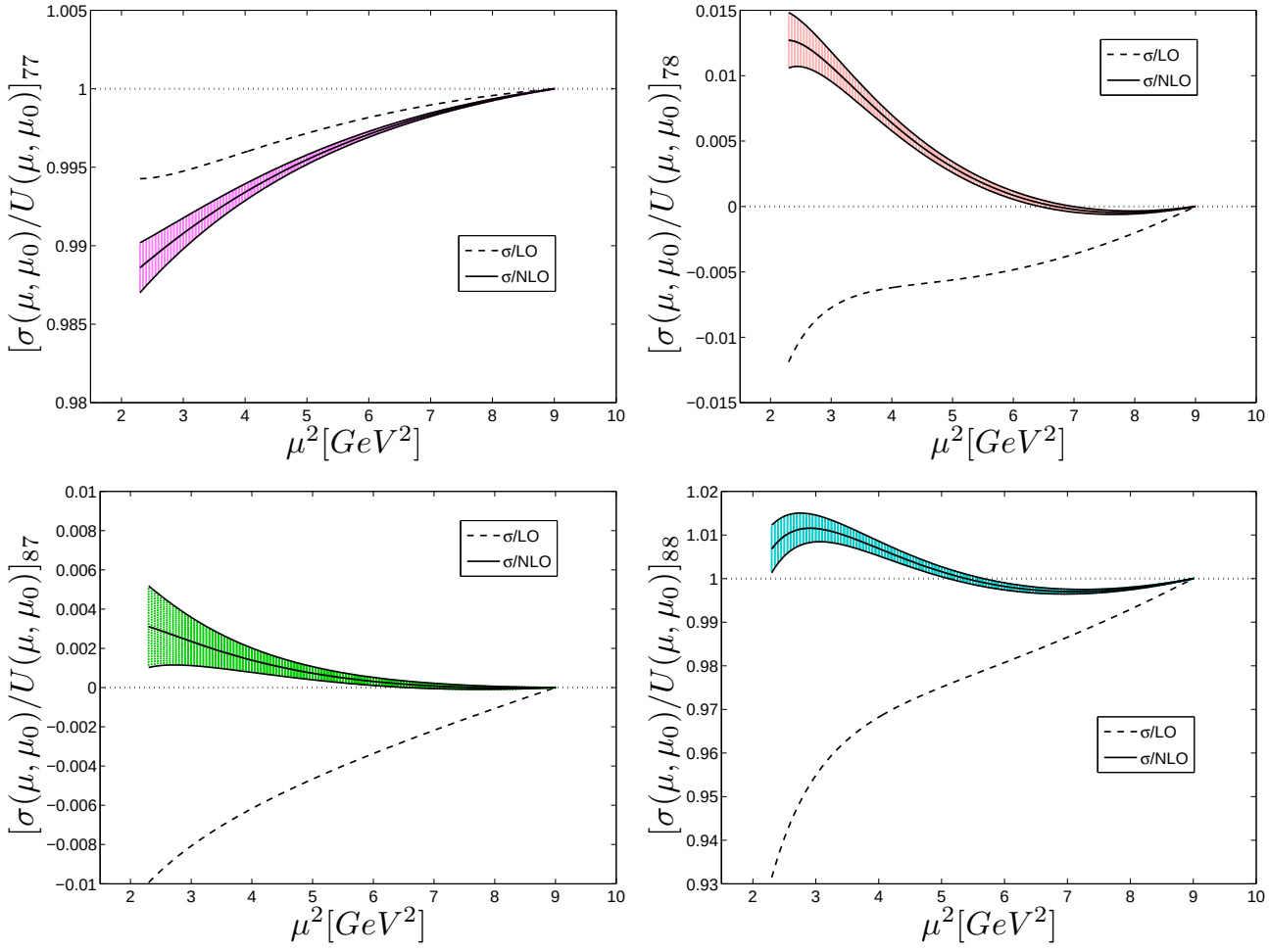

FIG. 7: Same as figure 5 for the step scaling matrix $\sigma(\mu,\mu_0)$ of the $(8,8)$ operators.

[1] M. Luscher et al., Nucl.Phys. B384 (1992) 168.
[2] S. Sint, Nucl.Phys. B421 (1994) 135.
[3] M. Luscher, P. Weisz and U. Wolff, Nucl. Phys. B359 (1991) 221.
[4] M. Luscher et al., Nucl. Phys. B389 (1993) 247.
[5] M. Luscher et al., Nucl. Phys. B413 (1994) 481.
[6] G. Martinelli et al., Nucl. Phys. B445 (1995) 81.
[7] M. Gorbahn and S. Jager, Phys. Rev. D82 (2010) 114001.
[8] L.G. Almeida and C. Sturm, Phys. Rev. D82 (2010) 054017.
[9] J.A. Gracey, Eur. Phys. J. C71 (2011) 1567.
[10] Y. Aoki et al., Phys. Rev. D78 (2008) 054510.
[11] C. Sturm et al., Phys. Rev. D80 (2009) 014501.
[12] R. Arthur and P. A. Boyle, Phys.Rev. D83 (2011) 114511.
[13] Y. Aoki et al., Phys.Rev. D84 (2011) 014503.
[14] S. Durr et al., JHEP 1108 (2011) 148.
[15] A. Gonzalez-Arroyo, J. Jurkiewicz and C. Korthals-Altes, (1981).
[16] A. Donini et al., Eur. Phys. J. C10 (1999) 121.
[17] Y. Zhestkov, (2001).
[18] M. Constantinou et al., JHEP 1008 (2010) 068.
[19] S. Durr et al., Phys.Lett. B705 (2011) 477.
[20] C. Sachrajda, PoS LATTICE2010 (2010) 018.
[21] L. Lellouch, (2011).
[22] R. Babich et al., Phys.Rev. D74 (2006) 073009.
[23] J. Wennekers, PoS LATTICE2008 (2008) 269.
[24] P. Dimopoulos et al., PoS LATTICE2010 (2010) 302.
[25] T. Blum et al., (2011), 1106.2714.
[26] L. Lellouch and M. Luscher, Commun.Math.Phys. 219 (2001) 31.
[27] E.J. Goode and M. Lightman, PoS LATTICE2010 (2010) 313.
[28] D. Renfrew et al., PoS LATTICE2008 (2008) 048.
[29] P.M. Vranas, Phys.Rev. D74 (2006) 034512.
[30] Y. Aoki et al., Phys.Rev. D83 (2011) 074508.
[31] C. Allton et al., Phys.Rev. D78 (2008) 114509.
[32] P. Boyle and N. Garron, PoS LATTICE2010 (2010) 307.
[33] D.B. Kaplan, Phys. Lett. B288 (1992) 342.
[34] Y. Shamir, Nucl. Phys. B406 (1993) 90.
[35] V. Furman and Y. Shamir, Nucl. Phys. B439 (1995) 54.
[36] M. Gockeler et al., Nucl. Phys. B544 (1999) 699.
[37] C. Lehner and C. Sturm, Phys.Rev. D84 (2011) 014001.
[38] P. Boyle, C. Jung and T. Wettig, (2003) THIT003.
[39] P. Boyle et al., Nucl.Phys.Proc.Suppl. 140 (2005) 169.
[40] T. Blum et al., Phys.Rev. D68 (2003) 114506.